THE JOURNAL OF PHYSICAL CHEMISTRY B
A JOURNAL OF THE AMERICAN CHEMICAL SOCIETY

pubs.acs.org/JPCB

Article

Pattern Recognition of Chemical Waves: Finding the Activation Energy of the Autocatalytic Step in the Belousov–Zhabotinsky Reaction

L. Howell, E. Osborne, A. Franklin, and É. Hébrard*

Cite This: J. Phys. Chem. B 2021, 125, 1667–1673

Read Online

ACCESS | Metrics & More | Article Recommendations

ABSTRACT: The Belousov–Zhabotinsky (BZ) reaction is an example of a homogeneous, nonequilibrium reaction used commonly as a model for the study of biological structure and morphogenesis. We report the experimental effects of temperature on spontaneously nucleated trigger waves in a quasi-two-dimensional BZ reaction–diffusion system, conducted isothermally at temperatures between 9.9 and 43.3 °C. Novel application of filter-coupled circle finding and localized pattern analysis is shown to allow the highly accurate extraction of average radial wave velocity and nucleation period. Using this, it is possible to verify a strong Arrhenius dependence of average wave velocity with temperature, which is used to find the effective activation energy of the reaction in accordance with predictions elaborated from the widely used Oregonator model of the BZ reaction. On the basis of our experimental results and existing theoretical models, the value for activation energy of the important self-catalyzed step in the Oregonator model is determined to be 86.58 ± 4.86 kJ mol^{-1}, within range of previous theoretical prediction.

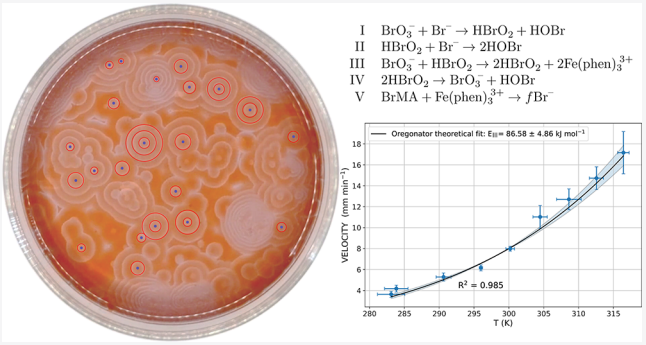

INTRODUCTION

The Belousov–Zhabotinsky (BZ) reaction is a chemical system commonly used to demonstrate the unusual dynamic behavior of homogeneous oscillating reactions. Such chemical clocks have been utilized as model systems for the periodicity observed in biological oscillators, for example, morphogenesis[1] and cardiac rhythms,[2] and have been investigated for their nonbiological applications such as wearable technology[3] and pressure sensors.[4] The classical BZ regime uses the reaction between bromate ions and an organic acid, mediated by a transition metal ion that acts as both a catalyst and indicator.[5,6] When conducted in quasi-two-dimensional conditions, such as a thin layer on the surface of a Petri dish, reaction and diffusion effects combine to form a variety of complex dynamic patterns and structures. These patterns arise as a result of two main and fundamentally different classes of chemical wave: trigger waves and pseudowaves.

This study focuses on the dynamics of trigger waves, gaining insight into reaction kinetics by investigating the effect of temperature on propagation velocity. This type of chemical wave is characterized by excited reaction–diffusion wavefronts seen as propagating bands of color that pass through the reaction medium and annihilate mutually upon contact.[7] In the case of the ferroin catalyzed BZ reaction, trigger waves are observed initially as a pattern of concentric blue rings, expanding from one or more nucleation points (Figure 1). These points can be initiated spontaneously or by an external perturbation, where localized oxidation of excitable orange $Fe(phen)_3^{2+}$ ions to blue $Fe(phen)_3^{3+}$ (where phen = phenanthroline in ferroin)[8] triggers the main reaction sequence.[7−9] Circular trigger waves then propagate radially from this point with constant velocity, creating "target pattern" structures as they are generated periodically from the center (Figure 1) until the reaction nears equilibrium.[9]

Several kinetic models of the BZ reaction have been created in an attempt to parametrize the complex reaction mechanism while retaining essential excitable and oscillatory behavior. Among these is the widely accepted Field, Körös, Noyes (FKN) mechanism[6] (Table 1), which encapsulates key equations and makes the reaction's fundamental autocatalysis and competing reactions explicit. Further, the Oregonator[10] (Table 2) is a five-step simplified model that succeeds in

Received: December 11, 2020
Revised: January 21, 2021
Published: February 3, 2021

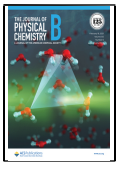

Figure 1. Aerial image of the ferroin catalyzed BZ reaction approximately 100 s after the first nucleation event. The reaction was conducted at 35 °C in a thin layer on a 14.2 cm diameter Petri dish. Trigger waves can be clearly seen as bands of blue, broken where adjacent wavefronts meet and mutually annihilate. Concentric "target pattern" structures form as chemical waves are generated periodically and propagate outward from central nucleation points. The reaction progression at 5× speed can be accessed at the following URL: https://www.youtube.com/watch?v=gbGxQ4yDSfc&t=0s ("Belousov−Zhabotinsky Reaction -7/2/19") as conducted in the Natural Sciences Undergraduate Teaching Lab at the University of Exeter by the authors.

retaining the principle elements of the FKN scheme while still showing good agreement with experimental data.[11]

Previous studies[12,13] have reported the activation energies of four of the five elemental steps in the Oregonator model; however the final activation energy relating to the third step of the model has proved challenging to determine and still remains uncertain. This energy, E_3, of the important autocatalytic step has been estimated theoretically to be between 83 and 113 kJ mol^{-1} using wave properties.[13] However, experimental support was previously lacking due to the challenges associated with accurately measuring trigger wave velocities. Previous experimental attempts suggest that wave velocity follows an Arrhenius relationship with temperature,[14] which can be used to determine the apparent activation energy of the reaction. However, existing work is limited by three factors: the number of trigger waves sampled, the accuracy of measurement methods, and the range of temperatures over which conclusions are drawn. Furthermore, existing works generally rely on measurement of single stimulated waves,[14] telling us little about the dynamic nature of the spontaneous patterns that make the reaction both beautiful and interesting.

In this paper, we report the effect of temperature on trigger wave velocity, conducting experiments between 9.9 and 43.3 °C which form physical limits for the spontaneous reaction. Image analyses using feature extraction and statistical techniques proposed here are shown to improve on previous analytical methods to determine wave velocity, allowing the robust extraction of trigger wave propagation velocities to a degree of accuracy not previously achieved. This allows the validation of the Arrhenius relationship and determination of a value for the missing activation energy E_3, in agreement with theoretical predictions.

Table 2. Oregonator Model,[10] Adapted Such That A = BrO_3^-, B = BrMA, P = HOBr, X = $HBrO_2$, Y = Br^-, Z = $Fe(phen)_3^{3+}$, and f = Stoichiometric Factor[13]

reaction	activation energy (kJ mol^{-1})
A + Y → X + P	E_1 [15] ≈ 54
X + Y → 2P	E_2 [15] ≈ 25
A + X → 2X + 2Z	E_3 [13] ≈ 83−113
2X → A + P	$E_{4.1}$ [16] ≈ 23
	$E_{4.2}$ [16] ≈ 18
B + Z → fY	E_5 [12] ≈ 70

METHODS

Experimental Procedure. All chemicals were sourced from Sigma-Aldrich (min 99% purity) with the exception of concentrated H_2SO_4 which was sourced from Fisher Chemicals (min 95% purity) and were used without further purification. Chemicals and equipment were supplied by the University of Exeter, U.K. The procedure for the ferroin catalyzed Belousov−Zhabotinsky reaction followed the protocol described by Winfree:[17]

Three stock solutions were prepared:

- A: 67 mL of deionized water; 2 mL of H_2SO_4, 5 g of $NaBrO_3$.
- B: 1 g of malonic acid dissolved in 10 mL of deionized water.
- C: 1 g of NaBr dissolved in 10 mL of deionized water.

12 mL of A, 2 mL of B, and 1 mL of C aliquots were combined in a 14.2 cm diameter Petri dish of liquid depth of approximately 1 mm. The mixture was swirled to mix and then left to react spontaneously. It was found that use of Triton X-100 surfactant caused the reaction solution to coagulate,

Table 1. FKN Mechanism[6] with MA = Malonic Acid[a]

$HOBr + Br^- + H^+ \rightarrow Br_2 + H_2O$	(1)
$HBrO_2 + Br^- + H^+ \rightarrow 2HOBr$	(2)
$BrO_3^- + Br^- + 2H^+ \rightarrow HBrO_2 + HOBr$	(3)
$2HBrO_2 \rightarrow BrO_3^- + HOBr + H^+$	(4)
$BrO_3^- + HBrO_2 + H^+ \rightarrow 2BrO_2^\bullet + H_2O$	(5)
$BrO_2^\bullet + H^+ + Ce^{3+} \rightarrow Ce^{4+} + HBrO_2$	(6)
$BrO_2^\bullet + Ce^{4+} + H_2O \rightarrow BrO_3^- + Ce^{3+} + 2H^+$	(7)
$Br_2 + MA \rightarrow BrMA + Br^- + H^+$	(8)
$MA + 6Ce^{4+} + 2H_2O \rightarrow 6Ce^{3+} + HCOOH + 2CO_2 + 6H^+$	(9)
$BrMA + 4Ce^{4+} + 2H_2O \rightarrow 4Ce^{3+} + Br^- + HCOOH + 2CO_2 + 5H^+$	(10)

[a]In the ferroin catalyzed reaction, Ce^{3+} and Ce^{4+} ions are replaced by $Fe(phen)_3^{2+}$ and $Fe(phen)_3^{3+}$.

https://dx.doi.org/10.1021/acs.jpcb.0c11079
J. Phys. Chem. B 2021, 125, 1667−1673

which distorted the "target pattern" structures produced; hence this was not used.

Temperature experiments were conducted in the range 9.9−43.3 °C at intervals of approximately 5 °C. These temperature extremes were found to be physical limits for investigation of the reaction. Below 9.9 °C resulted in nonexcitable media (no trigger waves observed), and at temperatures greater than ∼45 °C convection effects became significant and distorted the uniformity of the "target pattern" structures. To control temperature as the independent variable of investigation, all solutions and receptacles were adjusted to the required temperature using a hot plate or ice bath prior to combination and temperature was maintained throughout the experimental period. Temperature was monitored noninvasively across a 15 min recording period using a thermal imaging camera with precision of ±0.1 °C. Lighting conditions were optimized for overhead recording with a HD CCD camera using a white LED light ring to ensure uniform illumination and a blackout hood to prevent external changes in lighting conditions.

Image Analysis. In this study, combination image filtering techniques are used in conjunction with feature extraction to automatically and directly measure radii of expanding circles in the "target pattern" structures. This approach offers distinct advantages over traditional measurement of single stimulated waves, by allowing the rapid extraction of large pattern data sets and the accurate measurement of wave dynamics within spontaneously evolving systems. By use of this methodology, multiple "target pattern" structures can be detected as they form across the spatial confines of the dish and measured over the full course of the reaction. By utilization of statistical analyses of these large data sets extracted at a given temperature, robust conclusions regarding the spatial and temporal dynamics of trigger waves can be drawn. Parameters such as average radial wave velocity, wavelength, and nucleation period can be precisely determined, with low experimental uncertainty. In addition, we can investigate systemic variances in these values over the course of the reaction, commenting on the significance of these changes as the reaction nears equilibrium.

Extracting such trigger wave properties from the system is challenging, due to both the complexity of patterns and their dynamic nature. It is important to note that a secondary and fundamentally different class of wave, often called pseudo-waves, is also often observed experimentally. Although they can appear to propagate similarly to trigger waves, this type of wave represents bulk oscillations in ion concentration[18] rather than true reaction−diffusion behavior. As such, they have potential to disrupt the successful detection of trigger waves during algorithmic processing, and so their isolation and removal are an important step in preprocessing images prior to pattern detection. It was found that combination filtering with a Laplacian of Gaussian filter[19] and low threshold median filter served a dual purpose, for both isolating and removing pseudowaves and also for accentuating trigger wave fronts. The use of derivative filters is effective in enhancing contrast at trigger wavefront edges, and averaging filters remove excess noise.

Next, a form of the circle Hough transform technique[20] is used to detect the most prominent circles in the filtered images. This method accurately and consistently detects circles representing trigger waves in BZ "target pattern" structures, identifying the wavefront radii and nucleation points of up to 30 waves per image. This allows the rapid collection of a large data set with wavefront positions over time (Figure 2) which can be processed to characterize wave properties.

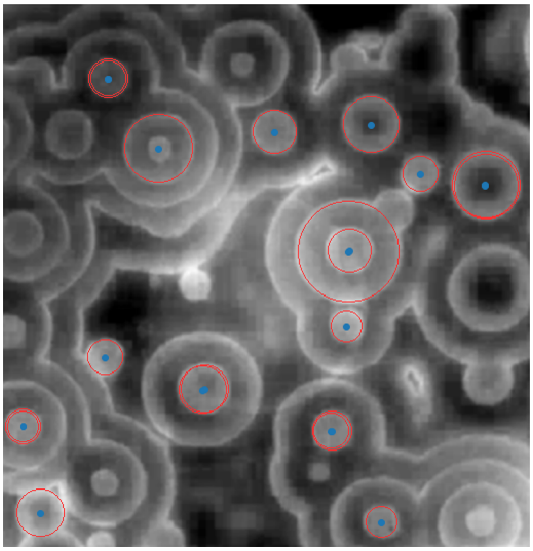

Figure 2. Sample result of trigger waves within "target pattern" structures in the 2D BZ reaction. Waves are detected using the Hough circle transform. The perimeter (red) and center (blue) are plotted on top of a grayscale, unfiltered image to demonstrate the applicability of circle finding to trigger wave measurement.

It is then possible to detect the position of nucleation sites in the images and to map the waves to their respective point of origin. This is achieved by identifying all circles with common center coordinates, within a fixed tolerance. The locations of nucleation points are fixed (unless annihilated by a higher-frequency "target pattern" structure), and thus all circles of common center must originate from the same nucleation site. In some images, several circles of different radii but common center may be detected, as is the concentric nature of the "target pattern" structures. Duplicate circles were suppressed by averaging radii of circles with both common center and radius. A density-based spatial clustering algorithm (DBSCAN)[21] was then applied to classify groups of points belonging to each specific wavefront with time. Trigger wave properties were finally determined using linear regression on each cluster of at least 10 data points. The gradient of each fitting function then gives the radial wave velocity, and the phase difference between adjacent waves gives the period for nucleation events (Figure 3).

This novel analysis method is shown to be both accurate and consistent in the extraction of wave properties from the spontaneous BZ reaction. Worst fit estimators give R^2 uncertainty from algorithmic processing less than 1% for all cases, suggesting that this methodology provides both an efficient and accurate method of determining the velocity of trigger waves from the "target pattern" structures in the BZ reaction.

RESULTS AND DISCUSSION

Previous work[5,12,22,23] has predominately investigated the relationship between trigger wave period/frequency and reaction temperature. Yet the experimental effects of temperature on wavefront velocity and hence pattern dynamics are largely limited. Past research[13,14] has suggested an Arrhenius

https://dx.doi.org/10.1021/acs.jpcb.0c11079
J. Phys. Chem. B 2021, 125, 1667−1673

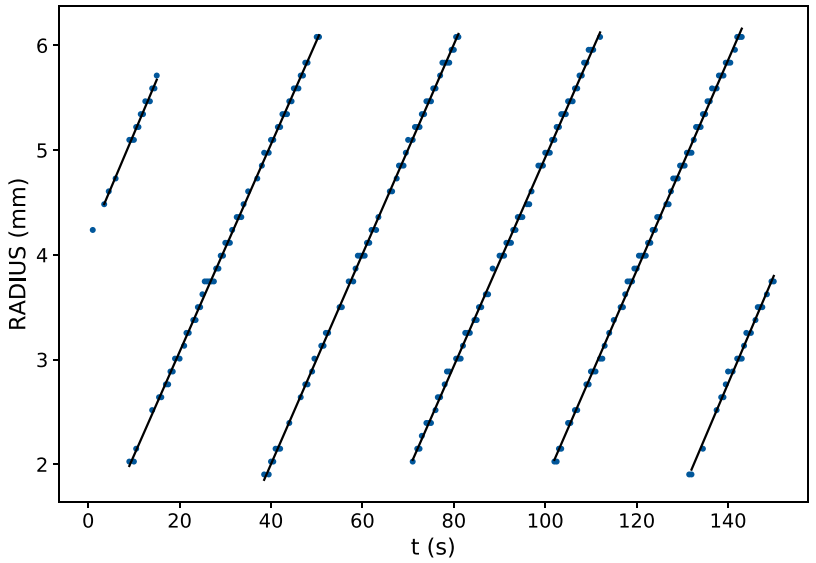

Figure 3. Radii of trigger waves (dark blue points) belonging to a single nucleation site in the BZ reaction conducted at 23 °C. DBSCAN clustering was used to identify the six groups belonging to separate waves. The gradient of linear regression (solid black lines) for each cluster gives the radial velocity of each wavefront, and the phase separation gives the nucleation period. Wave velocities are 0.1008 ± 0.0016 mm s^{-1}, with an R^2 value greater than 0.99 for each slope.

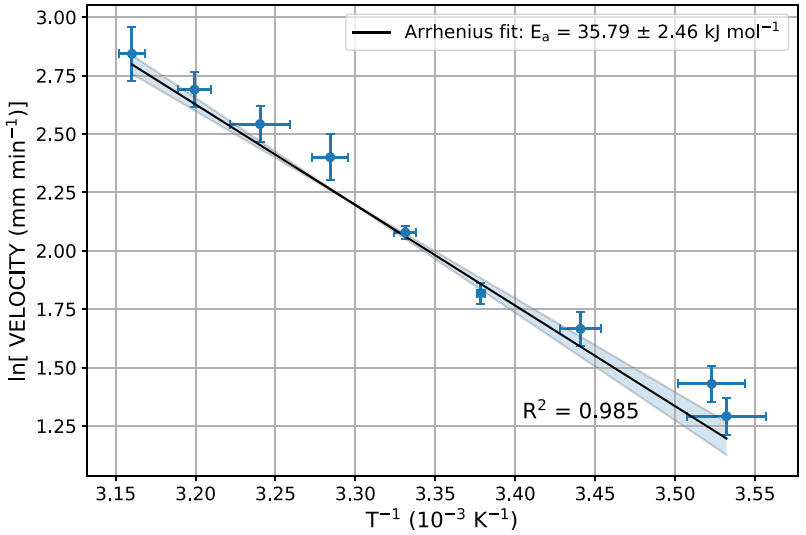

Figure 4. Arrhenius relationship between mean radial velocity and temperature for trigger waves in the BZ reaction. Vertical error bars show 1σ variation in radial velocity, and horizontal error bars show the uncertainty from temperature fluctuations as recorded by a thermal camera over the course of reaction. Orthogonal distance regression (solid) gives an apparent activation energy for the reaction E_a = 35.79 ± 2.46 kJ mol^{-1}, with a R^2 value of 0.985. The region of error from fitting is shown (light blue fill) between the worst fit estimators.

relationship between temperature and wave velocity v. Following Zhang et al.,[13] we assumed, for simplicity, a temperature independent pre-exponential factor A of the form

$$v \sim A\, e^{-E_a/(RT)} \quad (1)$$

where E_a is an apparent activation energy, R is the gas constant, and T is absolute temperature.

Using the filter-coupled circle detection analysis presented above, we are able to validate this relationship experimentally by measuring trigger waves formed spontaneously within reactions conducted between 9.9 and 43.3 °C. At each temperature, mean radial wave velocity and oscillation period are determined robustly by averaging measurements from the large number of trigger waves generated from several nucleation points over the course of the reaction. Nonlinear regression for the exponential form of the Arrhenius equation (eq 1) gives a R^2 coefficient of determination of 0.985, indicating that the average trigger wave velocity indeed exhibits a strong Arrhenius dependence with temperature (Figure 4). This fitting is achieved through orthogonal distance regression[24] to account for uncertainties in both the dependent and independent variables. The slope of the equation then gives an apparent activation energy for the reaction E_a = 35.79 ± 2.46 kJ mol^{-1}, which has been suggested to be linked to the autocatalytic production of bromous acid.[14] This value determined is within experimental uncertainty of previous literature values of 34.0 kJ mol^{-1} [14] and 34.9 ± 1.2 kJ mol^{-1}.[25]

It is also possible to gain valuable insight into the spatiotemporal behavior of the system at a given temperature by considering the set of wave velocities with their respective

https://dx.doi.org/10.1021/acs.jpcb.0c11079
J. Phys. Chem. B 2021, 125, 1667−1673

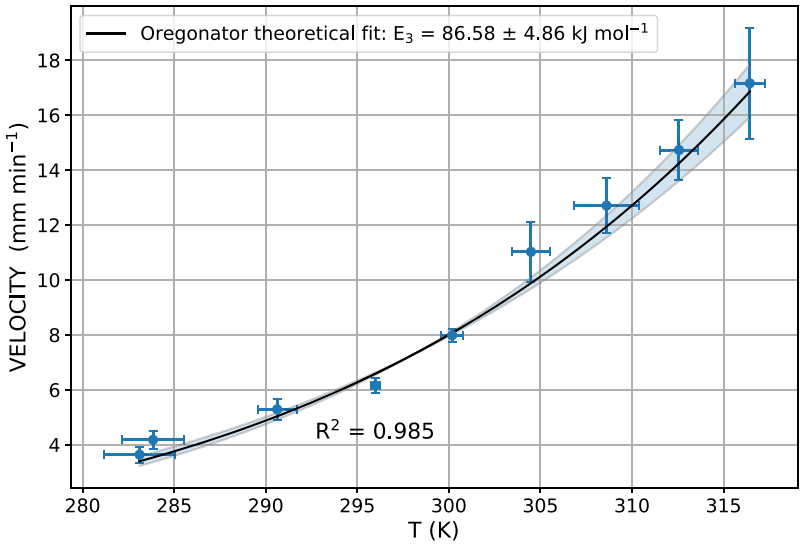

Figure 5. Oregonator theoretical fit for mean radial velocity of trigger waves as a function of system temperature. Vertical error bars show 1σ variation in radial wave velocity, and horizontal error bars show the uncertainty from temperature fluctuations in each experiment. Experimental data is fit to eq 2 using orthogonal distance regression with E_3 as the free parameter and c_0 = 0.121 10 mm s^{-1} (solid line). A strong functional fit is indicated by a R^2 value of 0.985, giving the activation energy E_3 = 86.58 ± 4.86 kJ mol^{-1} for the third step in the Oregonator model. The region of error from this fitting is shown (light blue fill) .

space and time coordinates. At constant temperature, trigger waves originating from single, spatially localized nucleation points were found to have a statistically low variation in velocities over the course of the reaction. At 23 °C, an average deviation of 1.66% from the mean was found for each nucleation site. This suggests that there is little change in wave velocity as the reaction progresses, in agreement with Zhabotinsky's original observations.[9]

Globally, however, taking wave speed from all nucleation points (over the spatial confines of the dish), the average deviation from the mean was found to be 4.62% at 23 °C implying a larger variation in wave velocity for fronts originating from different nucleation sites. As the measurement error due to algorithmic processing was shown to be small (less than 1%), the spread of wave velocities at constant temperature is the main source of uncertainty for average velocity measurements at each temperature. This variation may exist due to small inhomogeneities in the temperature distribution across the solution; those waves nucleated in "hotspots" of higher temperature have higher velocity, accentuated by the exponential relationship with temperature. These inhomogeneities may arise from experimental setup, as was observed in some thermal images, and are most significant at temperature extremes, where thermal flux is greatest.

Furthermore, the temperature dependence of trigger wave velocity can also be used to determine information about kinetic properties of the reaction. Crucially, the activation energy E_3 of the autocatalytic step in the widely used Oregonator model (Table 2) can be found. Using properties of the Oregonator model and diffusion equation, it can be shown that the propagation velocity v of an excitable trigger wave can be approximated by its relationship with the absolute temperature of the experimental system,[13] T_c. This is given by

$$v \approx c_0 \, e^{-\left(\frac{E_3+\sigma+E_a}{2R}\right)\left(\frac{1}{T_c}-\frac{1}{T_{c_0}}\right)} \quad (2)$$

where σ is the energy associated with the subexcitable boundary = −30 kJ mol^{-1}, E_a is the approximated energy associated with diffusion = 15 kJ mol^{-1}, R is the gas constant, c_0 = 0.121 10 mm s^{-1} is the trigger wave velocity at T_{c_0} = 298 K, and E_3 is the activation energy of the third reaction step in the Oregonator model. It is important to note that the value used here for the fixed parameter c_0 is around 1 order of magnitude larger than that used by Zhang et al.[13] and was calculated from the Arrhenius dependence shown in Figure 4. However, this value is supported by both analytical and empirical analysis, as wavefronts can be seen progressing by eye on the scale of several mm min^{-1}. By use of orthogonal distance regression,[24] this nonlinear model was fit to experimental data, giving the free parameter E_3 as 86.58 ± 4.86 kJ mol^{-1} (Figure 5) with a R^2 value equal to 0.985. This indicates a strong functional fit across the temperature range. The experimentally determined value for the activation energy of the autocatalytic step provides experimental conformation of previous estimates, narrowing the theoretical range of between 83 kJ mol^{-1} and 113 kJ mol^{-1}.[13] Estimates of this parameter have been used for many numerical and simulation models but previously lacked experimental backing. For example, a value in the range found by Zhang et al.[13] (84.5 kJ mol^{-1}) has been used by Barragán et al.[26] while applying the Oregonator to support the use of calorimetric studies as an alternative to previous analyte pulse perturbation (APP) techniques. In that study, the rate of entropy production was measured using the Oregonator model, with reactions occurring in a calorimeter and subject to a chemical pulse in the form of a Dirac delta function. For low analyte concentrations, a linear trend between entropy production due to heat transfer and the concentration of perturbing analyte was observed. This E_3 value is therefore important for further experimental and theoretical work in the field.

In addition to trigger wave propagation velocity, it is possible to extract the temporal oscillation period between nucleation of waves in "target pattern" structures. This was taken as the time between adjacent circles reaching a radius of 2 mm (Figure 3) and again could be investigated by statistical analysis over the space and time domains. Analysis shows that

https://dx.doi.org/10.1021/acs.jpcb.0c11079
J. Phys. Chem. B 2021, 125, 1667−1673

period and hence frequency also remain constant for a single nucleation point at constant temperature, averaging 2.03 ± 0.04 min^{-1} at 23 °C. The frequency of oscillations was found to increase approximately exponentially with temperature, as has been observed in the literature.[27] Chemical waves with constant frequency and velocity must, therefore, also have constant wavelength, as is apparent in "target pattern" structures. Since the wave velocity is constant, the wave profile is dependent only on a phase factor ϕ where $\phi = r - vt$. We therefore conclude that there is no dispersion in the system.

However, when the wavelength is analyzed over all nucleation points in space, much larger variation is observed, averaging 18% deviation from the mean across all temperatures. This suggests that in the spontaneous system, the wavelengths associated with different nucleation points can be very different at constant temperature. Experimentally, this is important to the pattern formation observed. As waves mutually annihilate upon contact, any aperiodicity in the system leads to unstable pattern formation. Higher frequency oscillations dominate, eventually taking over the surface of the Petri dish and forming increasingly compact and complex patterns with time.

CONCLUSIONS

This paper uses novel application of image analysis to accurately and precisely extract properties of trigger waves in the spontaneous, quasi-two-dimensional Belousov–Zhabotinsky reaction. Image filtering is coupled with feature extraction to detect and measure these propagating reaction–diffusion wavefronts in "target pattern" structures observed experimentally. Radius–time plots enable the determination of both trigger wave velocity and nucleation period, allowing robust characterization of wave behavior when averaged over large numbers of waves from the full reaction course. This method allows investigation of the effect of temperature on wave dynamics, validating the Arrhenius dependence of wave velocity and giving an apparent activation energy for the reaction of 35.79 ± 2.46 kJ mol^{-1}. In addition, a value for the activation energy of the previously uncertain third step of the Oregonator model was elucidated to be 86.58 ± 4.86 kJ mol^{-1}, narrowing the previously theoretical range. This value, which characterizes the autocatalytic step, furthers understanding of BZ reaction dynamics, with wider implications for modeling biological rhythms. Indeed, our results indicate that the "target pattern" wavefronts propagate at a constant velocity and could therefore be linked to nerve axon transmission as described by neuronal models such as the FitzHugh–Nagumo model.[28]

AUTHOR INFORMATION

Corresponding Author

É. Hébrard − *Astrophysics Group and Natural Sciences, University of Exeter, EX4 4QL Exeter, U.K.*; orcid.org/0000-0003-0770-7271; Email: e.hebrard@exeter.ac.uk

Authors

L. Howell − *Natural Sciences, University of Exeter, EX4 4QF Exeter, U.K.*

E. Osborne − *Natural Sciences, University of Exeter, EX4 4QF Exeter, U.K.*

A. Franklin − *Natural Sciences, University of Exeter, EX4 4QF Exeter, U.K.*

Complete contact information is available at: https://pubs.acs.org/10.1021/acs.jpcb.0c11079

Notes

The authors declare no competing financial interest.

ACKNOWLEDGMENTS

The authors wish to acknowledge the support of the Department of Natural Sciences of the University of Exeter, and all the staff and students involved in our second year module NSC2001 "Frontiers in Science 2", led by Dr. D. Horsell, through which this work was initially undertaken.

REFERENCES

(1) Turing, A. M. The Chemical Basis of Morphogenesis. *Philos. Trans. R. Soc. B* **1952**, *237*, 37–72.

(2) Murray, J. D. *Mathematical Biology: I. An Introduction*, 3rd ed.; Springer: Berlin, 2002.

(3) Fang, Y.; Yashin, V. V.; Dickerson, S. J.; Balazs, A. C. Detecting Spatial Defects in Colored Patterns Using Self-oscillating Gels. *J. Appl. Phys.* **2018**, *123*, 215107.

(4) Kuksenok, O.; Yashin, V. V.; Balazs, A. C. Mechanically Induced Chemical Oscillations and Motion in Responsive Gels. *Soft Matter* **2007**, *3*, 1138–1144.

(5) Körös, E. K. Monomolecular Treatment of Chemical Oscillation. *Nature* **1974**, *251*, 703–704.

(6) Field, R. J.; Körös, E.; Noyes, R. M. Oscillations in Chemical Systems. II. Thorough Analysis of Temporal Oscillation in Bromate-Cerium-Malonic Acid System. *J. Am. Chem. Soc.* **1972**, *94*, 8649–8664.

(7) Cross, M. C.; Hohenberg, P. C. Pattern Formation Outside of Equilibrium. *Rev. Mod. Phys.* **1993**, *65*, 851–1112.

(8) Ross, J.; Müller, S. C.; Vidal, C. Chemical Waves. *Science* **1988**, *240*, 460–465.

(9) Zaikin, A. N.; Zhabotinsky, A. M. Concentration Wave Propagation in Two-dimensional Liquid-phase Self-oscillating System. *Nature* **1970**, *225*, 535–537.

(10) Field, R. J.; Noyes, R. M. Oscillations in Chemical Systems. IV. Limit Cycle Behavior in a Model of a Real Chemical Reaction. *J. Chem. Phys.* **1974**, *60*, 1877–1884.

(11) Ren, J.; Gao, J.; Yang, W. Computational Simulation of Belousov-Zhabotinskii Oscillating Chemical Reaction. *Comput. Visualization Sci.* **2009**, *12*, 227–234.

(12) Ruoff, P. Antagonistic Balance in the Oregonator: About the Possibility of Temperature-Compensation in the Belousov Zhabotinsky Reaction. *Phys. D* **1995**, *84*, 204–211.

(13) Zhang, J.; Zhou, L.; Ouyang, Q. Estimation of the Activation Energy in the Belousov-Zhabotinsky Reaction by Temperature Effect on Excitable Waves. *J. Phys. Chem. A* **2007**, *111*, 1052–1056.

(14) Wood, P. M.; Ross, J. A Quantitative Study of Chemical Waves in the Belousov-Zhabotinsky Reaction. *J. Chem. Phys.* **1985**, *82*, 1924–1936.

(15) Kshirsagar, G.; Field, R. J. A Kinetic and Thermodynamic Study of Component Processes in the Equilibrium $5HOBr \rightleftharpoons 2Br_2 + BrO_3^- + 2H_2O + H$. *J. Phys. Chem.* **1988**, *92*, 7074–7079.

(16) Ágreda, B. J. A.; Field, R. J. Activation Energy for the Disproportionation of $HBrO_2$ and Estimated Heats of Formation of $HBrO_2$ and BrO_2. *J. Phys. Chem. A* **2006**, *110*, 7867–7873.

(17) Winfree, A. T. *The Geometry of Biological Time*, 1st ed.; Springer: Berlin, 1980.

(18) Winfree, A. Spiral Waves of Chemical Activity. *Science* **1972**, *175*, 634–636.

(19) Kong, H.; Akakin, H. C.; Sarma, S. E. A Generalized Laplacian of Gaussian Filter for Blob Detection and Its Applications. *IEEE Trans Cybern.* **2013**, *43*, 1719–1733.

(20) Yuen, H. K.; Princen, J.; Illingworth, J.; Kittler, J. Comparative Study of Hough Transform Methods for Circle Finding. *Image Vis Comput.* **1990**, *8*, 71–77.

(21) Ester, M.; Kriegel, H.; Sander, J.; Xu, X. A Density-Based Algorithm for Discovering Clusters in Large Spatial Databases with Noise. *KDD-96 Proc.* **1996**, 226–231.

(22) Pullela, S. R.; Cristancho, D.; He, P.; Luo, D.; Hall, K. R.; Cheng, Z. Temperature Dependence of the Oregonator Model for the Belousov-Zhabotinsky Reaction. *Phys. Chem. Chem. Phys.* **2009**, *11*, 4236−4243.
(23) Pullela, S. R.; Shen, J.; Marquez, M.; Cheng, Z. A Comparative Study of Temperature Dependence of Induction Time and Oscillatory Frequency in Polymer-immobilized and Free Catalyst Belousov-Zhabotinsky Reactions. *J. Polym. Sci., Part B: Polym. Phys.* **2009**, *47*, 847−854.
(24) Boggs, P. T.; Rogers, J. E. Orthogonal Distance Regression. *Statistical Analysis of Measurement Error Models and Applications*: Proceedings of the AMS-IMS-SIAM Joint Summer Research Conference, June 10−16, 1989; American Mathematical Society, 1990; p 186.
(25) Kuhnert, L.; Krug, H. J.; Pohlmann, L. Velocity of Trigger Waves and Temperature Dependence of Autowave Processes in the Belousov-Zhabotinsky Reaction. *J. Phys. Chem.* **1985**, *89*, 2022−2026.
(26) Barragán, D.; Ágreda, J.; Parra, W. Entropy Production in the Oregonator Model Perturbed in a Calorimeter with a Chemical Pulse. *J. Therm. Anal. Calorim.* **2015**, *119*, 705−713.
(27) Sen, S.; Riaz, S. S.; Ray, D. S. Temperature Dependence and Temperature Compensation of Kinetics of Chemical Oscillations; Belousov-Zhabotinskii Reaction, Glycolysis and Circadian rhythms. *J. Theor. Biol.* **2008**, *250*, 103−112.
(28) Nagumo, J.; Arimoto, S.; Yoshizawa, S. An Active Pulse Transmission Line Simulating Nerve Axon. *Proc. IRE* **1962**, *50*, 2061−2070.

https://dx.doi.org/10.1021/acs.jpcb.0c11079
J. Phys. Chem. B 2021, 125, 1667−1673